INTERNATIONAL JOURNAL FOR NUMERICAL METHODS IN ENGINEERING
Int. J. Numer. Meth. Engng. **44**, 535–550 (1999)

A MATHEMATICAL OPTIMIZATION METHODOLOGY FOR THE OPTIMAL DESIGN OF A PLANAR ROBOTIC MANIPULATOR

J. A. SNYMAN* AND D. F. BERNER

Structural Optimization Research Group, Department of Mechanical Engineering, University of Pretoria, Pretoria, 0002, South Africa

SUMMARY

A general optimization methodology for the optimal design of robotic manipulators is presented and illustrated by its application to a realistic and practical three-link revolute-joint planar manipulator. The end-effector carries out a prescribed vertical motion for which, respectively, the average torque requirement from electrical driving motors, and the electric input energy to the driving motors are minimized with respect to positional and dimensional design variables. In addition to simple physical bounds placed on the variables, the maximum deliverable torques of the driving motors and the allowable joint angles between successive links represent further constraints on the system. The optimization is carried out via a penalty function formulation of the constrained problem to which a proven robust unconstrained optimization method is applied. The problem of singularities (also known as degeneracy or lock-up), which may occur for certain choices of design variables, is successfully dealt with by means of a specially proposed procedure in which a high artificial objective function value is computed for such 'lock-up trajectories'. Designs are obtained that are feasible and practical with reductions in the objective functions in comparison to that of arbitrarily chosen infeasible initial designs. Copyright © 1999 John Wiley & Sons, Ltd.

KEY WORDS: optimization; optimal design; robot; manipulator; energy minimization; torque minimization

INTRODUCTION

In manufacturing the use of general purpose robots are not always very effective at carrying out any single task. The goal usually is to produce fairly similar products with minimal setup change and associated costs. To do this in a cost-effective manner, robots must be designed and optimized for a specific application(s) such that the tasks are performed in some optimal manner.[1] The objectives may, for example, be the attainment of high-accuracy motion, minimum transmission of vibration to the base, minimum stresses in the links, minimization of average or maximum torque requirement, minimum operational time or optimal energy usage. These objectives usually have to be achieved within certain constraints imposed by limitations on available construction materials, driving motors and other geometrical considerations.

Although much research has been done on the application of mathematical programming techniques to the optimum synthesis of mechanisms with respect to kinematic considerations,[2] surprisingly little work exists where the dynamics is also taken into account. An early

* Correspondence to: J. A. Snyman, Structural Optimization Research Group, Department of Mechanical Engineering, University of Pretoria, Pretoria, 0002, South Africa. E-mail: Jan.snyman@eng.up.ac.za

CCC 0029–5981/99/040535–16$17.50

Received 18 March 1997
Revised 7 May 1998

contribution in this direction is that of Sohoni and Haug,[3] who considered the dynamics of a four-bar mechanism in obtaining optimum designs with respect to, respectively, link cross-sections and counterweight placements. With regard to serial manipulators it appears that the optimal design of a robot manipulator, for even a simple task and where the dynamics is also taken into account, is very difficult.[4,5] Probable inhibiting factors are the extraordinary difficulty that the existence of singularities in the workspace represents[6] and the challenge of ensuring assembly of design during the application of mathematical optimization procedures.

Here a general optimization methodology for the optimal design of robotic manipulators, which perform a specific task(s), is presented and illustrated by its application to a three-link revolute-joint planar robotic manipulator. The end-effector carries out a prescribed vertical motion for which, respectively, the average torque requirement from the driving motors and the electric input energy to the driving motors are minimized with respect to positional and dimensional design variables. A trajectory optimization method is employed using a penalty function formulation of the problem to allow for physical constraints. Designs are obtained that are both feasible and practical with reductions in the objective function value in comparison to initial infeasible configurations.

GENERAL OPTIMIZATION METHODOLOGY

Assume that the trajectory of the end-effector of a general revolute-joint planar manipulator to perform a given task is prescribed, i.e. the position vector of a point on the effector as a function of time $\mathbf{r}(t)$ is prescribed over a time interval $[0, T]$. The trajectory $\mathbf{r}(t)$ may be analytically known or may be described in terms of spline functions fitted to data points. Inverse kinematics may now be applied to determine the link angle trajectories $\boldsymbol{\phi}(t)$ over $[0, T]$ which correspond to the prescribed end-effector trajectory $\mathbf{r}(t)$. Once $\boldsymbol{\phi}(t)$ is known inverse dynamics may be applied to obtain, for example, the torques $\boldsymbol{\tau}(t)$ that must be applied at the joints to give the desired link angle trajectories. With $\boldsymbol{\tau}(t)$ known different objective functions, which depend on these torques and are measures of the performance of the manipulator, such as, for example, overall transmission of reaction forces, maximum deflection amplitudes, average or maximum torque requirement, and total energy usage, may be computed. The values of the objective functions will, in general, depend on the design of the manipulator specified in terms of design variables. They may include the physical dimensions of the links, the positioning of the base relative to the trajectory, the mass distribution and the moments of inertia of the links, and the placement of driving motors.

One may now wish to vary the design variables so as to improve or optimize the performance of the manipulator. In doing so difficulties may arise because of the violation of specified physical constraints. In addition to the violation of simple physical bounds it may happen that for the given design the motion cannot be achieved because torques are required that exceed the maximum possible torques which can be provided by the motors. The design may also require the joint angles θ_i, between successive links, to exceed physical limitations imposed by the construction of the joints. Even worse, it may not be possible to assemble the manipulator for the given task because of a poor choice of the dimensional design variables. Another related serious problem that may occur is degeneracy or lock-up as the system moves along the prescribed trajectory. It should be clear that the optimization problem considered here is a particularly complicated constrained optimization problem. The major difficulty arises from the fact that the constraints, which relate to feasibility of assembly and lock-up, cannot always be precisely and analytically described. With the wide variety of constraints it is difficult to know the relative

weight each one carries. Nevertheless, it is proposed that the constrained problem be tackled by means of the formulation of a penalty function to which the proven robust unconstrained trajectory minimization procedure of Snyman[7,8] is applied. Special techniques are however required to deal with the assembly and lock-up constraints.

The application of the general optimization approach described above is now illustrated by its application to the vertical motion of a simple three link revolute-joint planar robotic manipulator. Although for illustrative purposes the example to be described is a relative simple one the methodology may, in principle, be easily extended to more complicated manipulators performing more intricate tasks with different objectives.

MODELLING OF THREE-LINK REVOLUTE-JOINT ROBOT

A schematic representation of the planar manipulator to be considered here is depicted in Figure 1. It consists of three links ($i = 1, 2, 3$), each of uniform mass per unit length connected to each other and to the base via revolute joints. The mass of each link is denoted by m_i, the length by ℓ_i and the moment of inertia about the z-axis through the centre of mass of the link by I_i. Three motors ($i = 1, 2, 3$) attached to the base and to links 1 and 2, drive links 1, 2 and 3, respectively. The different masses of the motors are denoted by M_i and moments of inertia about the centre of mass of the motor by J_i. The maximum torque that can be delivered by each motor is indicated by $\overline{\tau}_i$. The base joint is positioned at co-ordinates (x_b, y_b) relative to the indicated global co-ordinate system. An end-effector at the end-point of link 3 carries a payload of $L = 20$ kg weight. It is required that the manipulator lower the payload 1·273 m from A to B in 2 s. It is further required that link 3 remains horizontal throughout the vertical motion. The prescribed vertical trajectory that the endpoint must follow is defined by

$$\mathbf{r}(t) = \begin{bmatrix} x(t) \\ y(t) \end{bmatrix} = \begin{bmatrix} 0{\cdot}524 \\ 1{\cdot}505 + (2/\pi)(\cos(\pi/2)t - 1) \end{bmatrix} \tag{1}$$

for $t \in [0, T] = [0, 2\text{ s}]$.

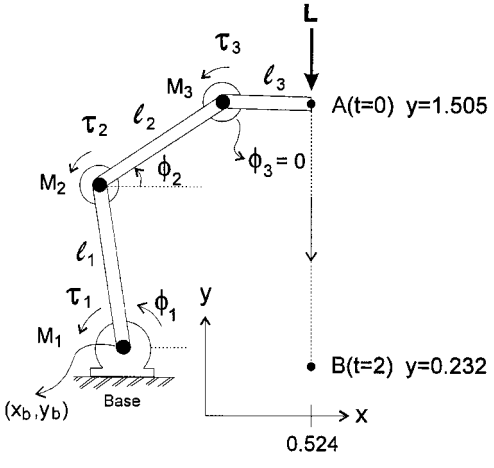

Figure 1. Schematic representation of planar manipulator

Table I. Motor characteristics

Motor i	M_i(kg)	$\overline{\tau}_i$(N m)	J_i(kg m^2)
1	8·5	2·1	0·0014
2	7·1	1·1	0·0011
3	3·7	0·5	0·0002

To ensure that the example be realistic and that a rigid-body approach may be followed in the analysis of the motion, the links are constructed of homogeneous circular hollow steel sections with a mass density of 17 kg m^{-1}.

This ensures that the maximum elastic deflection of the manipulator at the end-effector be less than 1 mm for the expected loading conditions. The mass and moment of inertia of each link i are obviously functions of ℓ_i. The moment of inertia of the payload L about its center of mass is 0·001 kg m^2.

The commercially available SEM permanent magnet d.c. motors are fixed directly onto the base and at the appropriate endpoints of link 1 and link 2. The motors drive the links through a gearbox of gear ratio 1 : 140. Motor and gear friction are ignored and the gears are assumed to be perfectly meshed and manufactured so that no backlash occurs. Further details concerning the individual masses M_i, the maximum allowable torques $\overline{\tau}_i$ and the moments of inertia J_i are given in Table I.

The inverse kinematic and dynamic analyses of the prescribed motion (1) are done numerically using the general Cartesian approach described by Nikravesh[9] and in which rigid bodies are assumed. For any given design the analyses yields numerical solutions for the time histories of the link angles $\boldsymbol{\phi}(t) = [\phi_1(t), \phi_2(t), \phi_3(t)]^T$ and of the corresponding torques $\boldsymbol{\tau}(t) = [\tau_1(t), \tau_2(t), \tau_3(t)]^T$ over the interval $[0, T]$.

THE OPTIMIZATION PROBLEM

The design variables

Here the objectives are to minimize (i) the average torque requirement and (ii) the electric input energy for the prescribed motion with respect to dimensional and positional design variables. The input energy is influenced by the torques which in turn are influenced by the link masses, moments of inertia and required accelerations. All these quantities are dependent on the link lengths ℓ_1, ℓ_2 and ℓ_3. Another factor that influences the torques is the base position (x_b, y_b) since the torques are also configuration dependent. Accordingly, the vector of design variables x chosen for this example is

$$\mathbf{x} = [x_1, x_2, x_3, x_4, x_5]^T = [\ell_1, \ell_2, \ell_3, x_b, y_b]^T \tag{2}$$

The objective functions

The objective function T_{av} corresponds to the average torque requirement and is explicitly defined by

$$T_{av}(\mathbf{x}) = \frac{1}{T}\int_0^T (|\tau_1(t)| + |\tau_2(t)| + |\tau_3(t)|)\,dt \tag{3}$$

To calculate the necessary electric input energy for the motion, the required input power to each motor is integrated over the time interval. The objective function E_{in} corresponding to the electric input energy is explicitly defined by

$$E_{\text{in}}(\mathbf{x}) = \int_0^T (P_1(t) + P_2(t) + P_3(t))\,\mathrm{d}t \tag{4}$$

where $P_i(t)$ denotes the required input power for motor i, $i = 1, 2, 3$.

The constraints

Each motor is limited to delivering a maximum torque $\overline{\tau}_i$. Therefore, the absolute value of the torque $\tau_i(t)$ that the motor is required to deliver at any instant t during the motion $[0, T]$ must not exceed the maximum deliverable value $\overline{\tau}_i$. Mathematically these *torque constraints* may be stated as follows:

$$g_i(\mathbf{x}) \equiv \int_0^T c_i(t)\,\mathrm{d}t \leqslant 0, \quad i = 1, 2, 3 \tag{5}$$

where $c_i(t) = |\tau_i(t)| - \overline{\tau}_i$ if $|\tau_i(t)| \geqslant \overline{\tau}_i$, otherwise $c_i(t) \equiv 0$.

Due to the way the links are connected at the joints and the mounting of motors near the joints, only a certain range of joint angles between two successive links are physically possible. Figure 2 shows two coupled adjacent links and indicates that the joint angle θ cannot be smaller than $\theta_{\min}$ and not greater than $\theta_{\max}$.

Mathematically these *joint angle constraints* may be expressed as

$$g_i(\mathbf{x}) \equiv \int_0^T d_j(t)\,\mathrm{d}t + \int_0^T e_j(t)\,\mathrm{d}t \leqslant 0, \quad i = 4, 5, 6; \quad j = i - 3 \tag{6}$$

where for joints $j = 2, 3$ ($i = 5, 6$), $d_j(t) = |\theta_j(t)| - \theta_{\max}$ if $|\theta_j(t)| > \theta_{\max}$, otherwise $d_j(t) \equiv 0$; and $e_j(t) = \theta_{\min} - |\theta_j(t)|$ if $|\theta_j(t)| < \theta_{\min}$, otherwise $e_j(t) \equiv 0$, and where $\theta_{\max} = 5\pi/3$ rad and $\theta_{\min} = \pi/3$ rad. Satisfaction of these conditions ensures that the joint angle limits are never exceeded throughout the time interval $[0, T]$ of the motion. Figure 3 depicts the restriction for the base joint angle θ_1. For practical reasons it is prescribed that this joint angle cannot lie in the range of $4\pi/3$ to $5\pi/3$ rad. Therefore for $i = 4$, $j = 1$ in (6): if $\theta_1 < 0$ then if $\theta_1 < -\pi/3$ set $d_1 = -\theta_1 - \pi/3$, otherwise set $d_1 \equiv 0$; else if $\theta_1 > 0$ then if $\theta_1 > 4\pi/3$ set $d_1 = \theta_1 - 4\pi/3$, otherwise set $d_1 \equiv 0$; $e_1 \equiv 0$ for all θ_1.

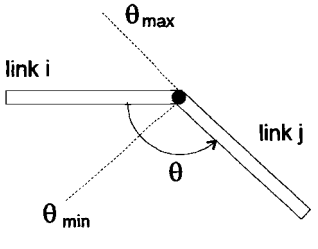

Figure 2. Coupled adjacent links

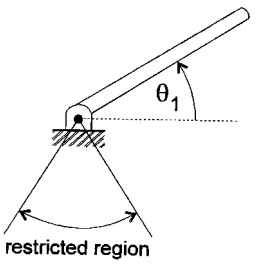

Figure 3. Base joint angle

Simple bounds are placed on the lengths of the links to ensure sufficient space for the placement of an end-effector device, such as a gripper, to the last link and for the mounting of motors and gear boxes to the other links. Furthermore, a *positional constraint* is imposed on the placement of the x-position of the base. The explicit constraints with lengths and position specified in meters are

$$g_7(\mathbf{x}) \equiv 0{\cdot}25 - \ell_1 \leqslant 0 \tag{7}$$

$$g_8(\mathbf{x}) \equiv 0{\cdot}25 - \ell_2 \leqslant 0 \tag{8}$$

$$g_9(\mathbf{x}) \equiv 0{\cdot}15 - \ell_3 \leqslant 0 \tag{9}$$

$$g_{10}(\mathbf{x}) \equiv x_b - 0{\cdot}3 \leqslant 0 \tag{10}$$

It may happen that due to an initial poor estimate of the design variables, or due to adjustment of the variables in the optimization process, that the robot is not physically able to reach all points on the prescribed path. In an attempt to prevent this from happening one may set down *assembly constraints*. Inspection of Figure 1 shows that starting point A and end position B represent two critical configurations. To ensure assembly with the end-effector reaching both points, with link 3 horizontal, the variables must satisfy the following two constraints:

$$g_{11}(\mathbf{x}) \equiv (1{\cdot}505 - y_b)^2 + (0{\cdot}524 - \ell_3 - x_b)^2 - (\ell_1 + \ell_2)^2 \leqslant 0 \tag{11}$$

$$g_{12}(\mathbf{x}) \equiv (0{\cdot}232 - y_b)^2 + (0{\cdot}524 - \ell_3 - x_b)^2 - (\ell_1 + \ell_2)^2 \leqslant 0 \tag{12}$$

Satisfaction of condition (11) ensures feasibility at the start and allows for commencement of the analysis of the motion for the selected set of design variables. On the other hand (12) guarantees feasibility of motion at the end of the time interval.

Degeneracy

In spite of the satisfaction of conditions (11) and (12) it may still happen that *degeneracy* or *lock-up* occurs at some intermediate point along the path between A and B, making the computation of $T_{av}(\mathbf{x})$ and $E_{in}(\mathbf{x})$ impossible. In general it is not easy to specify in advance at what point and under what general geometrical conditions degeneracy will occur. It is therefore necessary to adopt a special procedure if degeneracy occurs along the integration path.

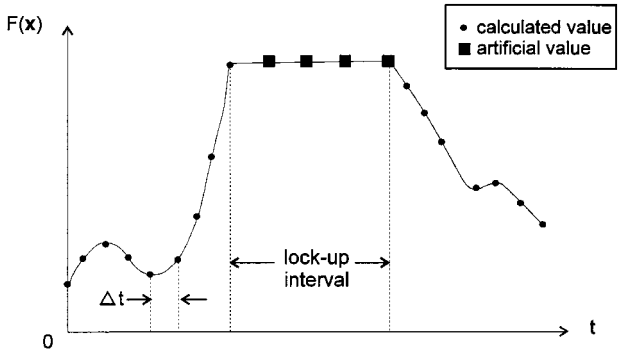

Figure 4. Numerically computed objective function for a 'lock-up trajectory'

It is well known[10] that as a mechanical system approaches a lock-up configuration the torques will appear to increase without bounds. In practice, the analysis is done at discrete-time intervals Δt. If the system is now forced through the lock-up position and the analysis continued for the prescribed path, the analysis will fail at intermediate steps where assembly is no longer possible. However, as assembly at position B is guaranteed by satisfaction of condition (12), a point will be reached where assembly is again possible and the analysis can successfully be continued. The following heuristic procedure is now proposed to deal with such a 'lock-up trajectory'. At the integration points t where assembly fails set $\tau_i(t) = \tau_i(t_s)$, where t_s is the last step at which assembly was successfully carried out. Use these values in the numerical integration of (3) and (4) to give an artificial value for the objective function. This situation is depicted in Figure 4. Since one expects the values of $\tau_i(t_s)$ to be relatively large the computed value for T_{av} and E_{in} will be very high. Also, the longer the non-assembly time interval, and therefore the more serious the lock-up situation, the larger the expected value for the objective function. A good optimization procedure for the minimization of the objective function should, if the above integration procedure is adopted which gives a relative high objective function value for a 'lock-up trajectory', drive the design away from such an undesirable situation.

In summary, the optimization problem reduces to:

$$\begin{aligned} &\text{minimize} \quad F(\mathbf{x}) \\ &\text{subject to } g_i(\mathbf{x}) \leqslant 0, \quad i = 1, 2, \ldots, 12 \end{aligned} \tag{13}$$

where $F(\mathbf{x})$ represents the objective function, either $T_{av}(\mathbf{x})$ or $E_{in}(\mathbf{x})$, to be minimized. Allowance is made for the computation of an artificial objective function value for choices of design variables that result in 'lock-up trajectories'. The optimum value of $\mathbf{x}$ is denoted by $\mathbf{x}^*$.

OPTIMIZATION PROCEDURE

The optimization problem is solved numerically by applying an unconstrained optimization method to a penalty function formulation of constrained problem (13). This is the most simple and straightforward approach to the handling of constrained optimization problems. It requires however a robust optimization algorithm. The method employed here is the dynamic trajectory method of Snyman[7,8] as modified by Berner.[11] This gradient method is a proven robust method

that differs conceptually from other gradient methods in that no explicit line searches are performed. It approaches the minimization problem by considering the trajectory of a particle of unit mass in a conservative force field of dimension equal to the number of variables, and where the function to be minimized represents the potential energy of the particle. An interfering strategy is adopted in which the particle is systematically forced to lose energy and to converge to a local minimum. The method has successfully been applied to penalty function formulated constrained problems.[12,13]

The nature of the dynamic trajectory method is ideally suited to the current problem. Since the objective function and gradients are computed numerically, and in particular because discontinuities may be present in the artificial objective function when lock-up occurs (see discussion under *Degeneracy* in the previous section), the objective function may contain random and local inaccuracies and fluctuations. In effect the function contains 'noise'. It has been shown that in such cases, where standard and more classical optimization methods fail, the dynamic trajectory method, being more robust is successful.[14,15] The trajectory method generates a minimization path that is relatively insensitive to local inaccuracies and discontinuities in the gradients, passing over local ripples in the objective function. In particular it moves away from regions of relative high objective function value, corresponding to lock-up situations, to areas of lower function value where the behaviour is more smooth.

The appropriate penalty function for the current problem is

$$P(\mathbf{x}) = F(\mathbf{x}) + \sum_{i=1}^{12} \beta_i g_i(\mathbf{x})^2 \tag{14}$$

where $\beta_i \equiv 0$ if $g_i(\mathbf{x}) \leqslant 0$, otherwise $\beta_i = \rho$ where ρ is some suitably large positive penalty parameter. In the application of Snyman's trajectory method the value of the parameter $\rho = \rho_k$ at each step k along the optimization trajectory is systematically increased by setting $\rho = \rho_k = \mu\rho_{k-1}$. Here μ is a magnification factor slightly larger than one and starts with a relative small value for ρ_1. In this way, ρ is slowly increased up to a maximum value $\rho_{\max}$ (see References 12 and 13). This results in a smooth trajectory leading to the neighbourhood of a constrained local minimum. Typically, the choice $\mu = 1{\cdot}03$, $\rho_1 = 1$ and $\rho_{\max} = 10^7$ is made.

A serious and unusual problem arises however if constraints $i = 11$ and/or $i = 12$ (see (11) and (12)) are violated. If this happens then either no initial assembly or no final assembly is feasible, or both are not feasible, and it is not possible to compute $F(\mathbf{x})$ and therefore $P(\mathbf{x})$ in (14). It is therefore proposed that if any of these constraints are violated then $F(\mathbf{x})$ and all the constraints, except the assembly constraints (11) and (12), are simply ignored and $P(\mathbf{x})$ is replaced by

$$\bar{P}(\mathbf{x}) = \sum_{i=11}^{12} \beta_i g_i(\mathbf{x})^2 \tag{15}$$

and the minimization trajectory continued until return to the region in which both assembly conditions are satisfied is achieved. At this point the algorithm reverts to considering the full penalty function (14). Again, it must be mentioned that such switching, which of course results in discontinuities, cannot in general be handled by standard classical optimization methods. Since analytic expressions for the torque and for some of the constraints are not available use have to be made of finite differences in the computation of the necessary gradients. This unfortunately leads to a significant increase in computational time.

Convergence to the optimum design $\mathbf{x}^*$ is assumed if the norm of the immediate and average change over the previous five steps in the design vector becomes less than 0·1 mm.

NUMERICAL RESULTS

The computations were done on a 486 DX 66 MHz personal computer. An integration time step $\Delta t = 0{\cdot}008$ s was used in the evaluation of integrals (3) and (4). For the computation of the finite difference gradients a step size of 10^{-5} was used throughout. The optimization algorithm was successful in obtaining optimum solutions for both the minimization of the average motor torque requirement and the minimization of the electric input energy to the motors. For interest sake, and to illustrate the generality and flexibility of the approach and also the influence of constraints, the optimization was carried out in both cases of the objective function with and without the imposition of joint angle constraints. All the results listed in the tables are to the nearest millimeter, Joule and thousandth of a Newton-meter

The four configurations shown in Figure 5 were used as initial starting points for the minimization of both the objective functions. None one of these configurations is feasible since all of them have torque and/or joint angle constraints violated. See Tables II–V.

The initial design vector $\mathbf{x}^0$ for cases 1a and 1b is the same but the initial configurations are in fact different because of the two different possible choices for the initial joint angle between link 1 and link 2 as is apparent from Figure 5. The same applies for configurations 2a and 2b.

Minimization of the average motor torque requirement without joint angle constraints

Figure 6 shows the optimum solution obtained for the minimization of the average required motor torque when joint angle constraints are ignored. All the initial designs go to the same optimum solution $\mathbf{x}^*$.

Here it is interesting to note that the y co-ordinate of the base position corresponds to the midpoint of the path. For the optimum solution all the imposed constraints are satisfied. Table II shows the detailed results obtained for this example. This solution is still infeasible from a joint angle point of view and it remains therefore to explicitly introduce the joint angle constraints.

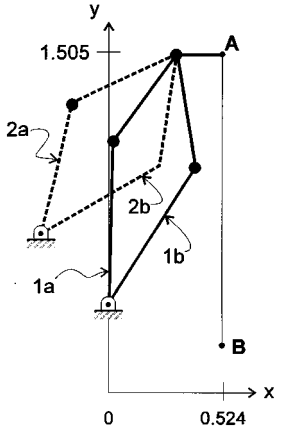

Figure 5. Initial designs

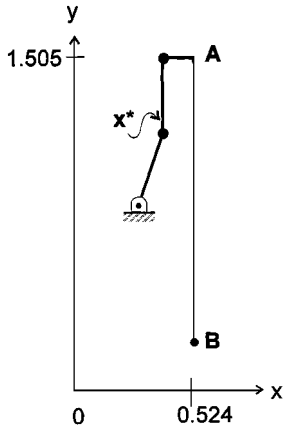

Figure 6. Average torque minimizing configurations without joint angle constraints

Table II. Results for the minimization of the average torque requirement without joint angle constraints

Initial design	1a	1b	2a	2b
$x^0 = \ell_1$	0·7	0·7	0·6	0·6
ℓ_2	0·5	0·5	0·5	0·5
ℓ_3	0·20	0·2	0·2	0·2
x_b	0·0	0·0	− 0·3	− 0·3
y_b	0·4	0·4	0·7	0·7
$T_{av}(\mathbf{x}^0)$	2·304	2·211	3·198	3·214
Violated constraints	$g_1 = 0{\cdot}014$	—	$g_1 = 0{\cdot}353$	$g_1 = 0{\cdot}093$
	$g_2 = 0{\cdot}093$	—	$g_2 = 0{\cdot}067$	$g_2 = 0{\cdot}210$
$\mathbf{x}^* = \ell_1$	0·307	0·313	0·313	0·314
ℓ_2	0·335	0·329	0·329	0·328
ℓ_3	0·150	0·150	0·150	0·150
x_b	0·300	0·300	0·300	0·300
y_b	0·869	0·869	0·869	0·869
$T_{av}(\mathbf{x}^*)$	1·065	1·064	1·064	1·064
Violated constraints	—	—	—	—
no. of iterations	603	608	688	641

Minimization of the average motor torque requirement with additional joint angle constraints

Figure 7 shows the two local optimum solutions obtained for the minimization of the average motor torque requirement with additional joint angle constraints. Here interestingly, configurations with the same initial design vectors but different in sense, i.e. both the 'left elbow' and 'right elbow' initial configurations converge to the same local optimum solution. Initial designs 1a and 1b go to $\mathbf{x}_1^*$ and initial designs 2a and 2b to $\mathbf{x}_2^*$.

Both solutions are feasible with all the constraints satisfied. The overall optimum solution for the minimization of the average motor torque requirement with all the constraints imposed is taken as $\mathbf{x}_1^*$ because its objective function value is the lowest of the two local optima. Table III

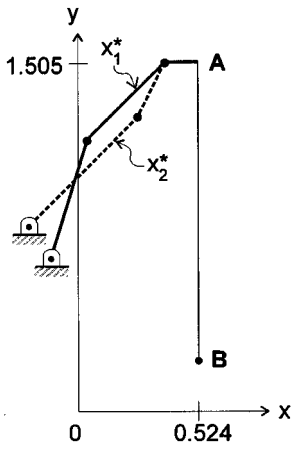

Figure 7. Average torque minimizing configurations with all constraints imposed

Table III. Results for the minimization of the average torque requirement with joint angle constraints

Initial design	1a	1b	2a	2b
$\mathbf{x}^0 = \ell_1$	0·7	0·7	0·6	0·6
ℓ_2	0·5	0·5	0·5	0·5
ℓ_3	0·20	0·2	0·2	0·2
x_b	0·0	0·0	− 0·3	− 0·3
y_b	0·4	0·4	0·7	0·7
$T_{av}(\mathbf{x}^0)$	2·304	2·211	3·198	3·214
Violated constraints	$g_1 = 0{\cdot}014$	$g_3 = 0{\cdot}036$	$g_1 = 0{\cdot}353$	$g_1 = 0{\cdot}093$
	$g_2 = 0{\cdot}093$	$g_4 = 0{\cdot}506$	$g_2 = 0{\cdot}067$	$g_2 = 0{\cdot}210$
	$g_4 = 0{\cdot}506$	$g_5 = 0{\cdot}183$	—	$g_3 = 0{\cdot}146$
	$g_5 = 0{\cdot}078$	—	—	—
$\mathbf{x}^* = \ell_1$	0·518	0·518	0·658	0·654
ℓ_2	0·462	0·447	0·250	0·250
ℓ_3	0·150	0·150	0·150	0·150
x_b	− 0·119	− 0·112	− 0·205	− 0·195
y_b	0·669	0·673	0·806	0·815
$T_{av}(\mathbf{x}^*)$	2·368	2·362	2·473	2·474
Violated constraints	—	—	—	—
no. of iterations	802	682	1496	591

shows the detailed results obtained for all the initial starting configurations. As expected the imposition of additional joint angle constraints increases the optimum function value.

Minimization of the electric input energy without joint angle constraints

Figure 8 shows two optimum solutions obtained for the minimization of the electric input energy to the motors when joint angle constraints are ignored. Here initial configurations of

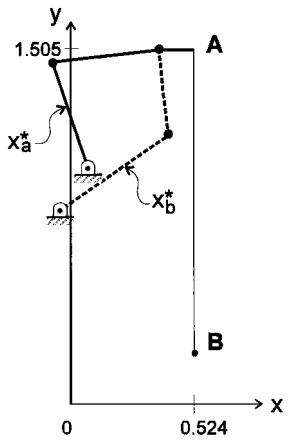

Figure 8. Energy minimizing configurations without joint angle constraints

Table IV. Results for the minimization of the electric input energy to the driving motors without joint angle constraints

Initial design	1a	1b	2a	2b
$\mathbf{x}^0 = \ell_1$	0.7	0.7	0.6	0.6
ℓ_2	0·5	0·5	0·5	0·5
ℓ_3	0·20	0·2	0·2	0·2
x_b	0·0	0·0	− 0·3	− 0·3
y_b	0·4	0·4	0·7	0·7
$E_{in}(\mathbf{x}^0)$	854	742	777	821
Violated constraints	$g_1 = 0{\cdot}014$	—	$g_1 = 0{\cdot}353$	$g_1 = 0{\cdot}093$
	$g_2 = 0{\cdot}093$	—	$g_2 = 0{\cdot}067$	$g_2 = 0{\cdot}210$
$\mathbf{x}^* = \ell_1$	0·488	0·562	0·486	0·566
ℓ_2	0·466	0·364	0·468	0·364
ℓ_3	0·150	0·150	0·150	0·150
x_b	0·068	− 0·033	0·076	− 0·040
y_b	0·988	0·828	0·996	0·832
$E_{in}(\mathbf{x}^*)$	635	660	635	660
Violated constraints	—	—	—	—
no. of iterations	854	654	929	654

similar sense converge to the same optimum solution. Initial 'left elbow' designs 1a and 2a go to $\mathbf{x}_a^*$ and initial 'right elbow' designs 1b and 2b to $\mathbf{x}_b^*$.

Both designs are feasible with respect to the imposed constraints. The overall optimum solution for the minimization of the electric input energy without joint angle constraints imposed is taken as $\mathbf{x}_a^*$ because its objective function value is the lowest of the two local optima. Table IV shows the detailed results obtained for all the initial starting configurations. These solutions are however still infeasible from a joint angle point of view and it remains therefore to explicitly introduce the joint angle constraints.

Minimization of the electric input energy with additional joint angle constraints

Figure 9 shows the two optimum solutions obtained for the minimization of the electric input energy to the motors with joint angle constraints imposed. Similar 'elbow' initial configurations converge to the same local optimum solution. Initial designs 1a and 2a go to $\mathbf{x}_a^*$ and initial designs 1b and 2b to $\mathbf{x}_b^*$.

Both solutions are feasible. The overall optimum solution to the minimization of the electric input energy to the motors with all the constraints imposed is given by $\mathbf{x}_a^*$. Table V shows the

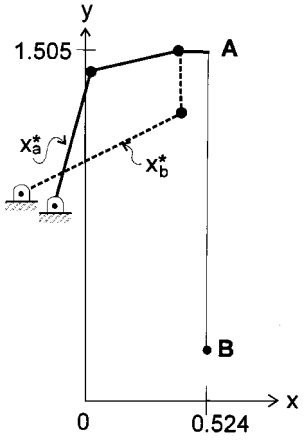

Figure 9. Energy minimizing configurations with all the constraints imposed

Table V. Results for the minimization of the electric input energy to the driving motors with joint angle constraints

Initial design	1a	1b	2a	2b
$\mathbf{x}^0 = \ell_1$	0·7	0·7	0·6	0·6
ℓ_2	0·5	0·5	0·5	0·5
ℓ_3	0·20	0·2	0·2	0·2
x_b	0·0	0·0	− 0·3	− 0·3
y_b	0·4	0·4	0·7	0·7
$E_{in}(\mathbf{x}^0)$	854	742	777	821
Violated constraints	$g_1 = 0{\cdot}014$	$g_3 = 0{\cdot}036$	$g_1 = 0{\cdot}353$	$g_1 = 0{\cdot}093$
	$g_2 = 0{\cdot}093$	$g_4 = 0{\cdot}506$	$g_2 = 0{\cdot}067$	$g_2 = 0{\cdot}210$
	$g_4 = 0{\cdot}506$	$g_5 = 0{\cdot}183$	—	$g_3 = 0{\cdot}146$
	$g_5 = 0{\cdot}078$	—	—	
$x^* = \ell_1$	0·576	0·681	0·576	0·681
ℓ_2	0·391	0·256	0·391	0·256
ℓ_3	0·150	0·150	0·150	0·150
x_b	− 0·134	− 0·221	− 0·134	− 0·221
y_b	0·862	0·877	0·862	0·879
$E_{in}(\mathbf{x}^*)$	666	711	666	711
Violated constraints	—	—	—	—
no. of iterations	802	815	874	820

detailed results obtained for all the initial starting configurations. Here interestingly the satisfaction of the additional joint angle constraints does not increase the optimum energy value to the same dramatic extent as in the case of the minimization of the torque requirement (see Tables II and III).

DISCUSSION OF RESULTS

It is clear from the results that the proposed optimization methodology is capable of finding a satisfactory optimum design, *provided such a feasible solution exists* for the particular choice of electric motors. It is found that if too small motors are used at first, no feasible design is found. It is also evident that all the practical constraints should be imposed simultaneously to ensure a feasible design. The results show that the prescribed optimization methodology represents an effective design tool by means of which different link and motor combinations may be assessed with respect to feasibility and optimality.

The success of the algorithm in finding a satisfactory optimum design from a poor initial design is clearly indicated in Table III for the minimization of the average torque requirement for initial designs 1a and 1b. Although the algorithm moves to a design with a higher objective function value, the optimum design is a feasible one as opposed to the infeasible initial ones. Overall the handling of violated constraints is very satisfactory as is illustrated in Figure 10 for case 2a in Table V. The figure shows the torque vs. time graph of the first motor for initial design 2a and for the optimum solution $\mathbf{x}_a^*$. It clearly shows that the required torque for the optimum solution is within the allowable limits throughout the motion.

Similarly Figure 11 shows how, for case 1a in Table V, the algorithm succeeds in handling joint angle constraint violations. The figure shows the joint angle vs. time graph for joint 2 for both the initial configuration 1a and the optimum $\mathbf{x}_a^*$.

The study emphasizes the importance of the use of different starting designs in finding a true optimum solution of the problem. The results show that using different starting points,

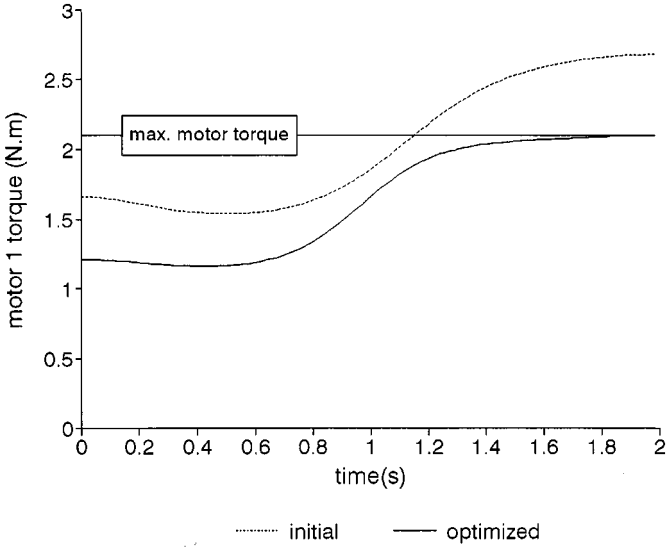

Figure 10. Torque vs. time graph of motor 1 (Case 2a, Table V)

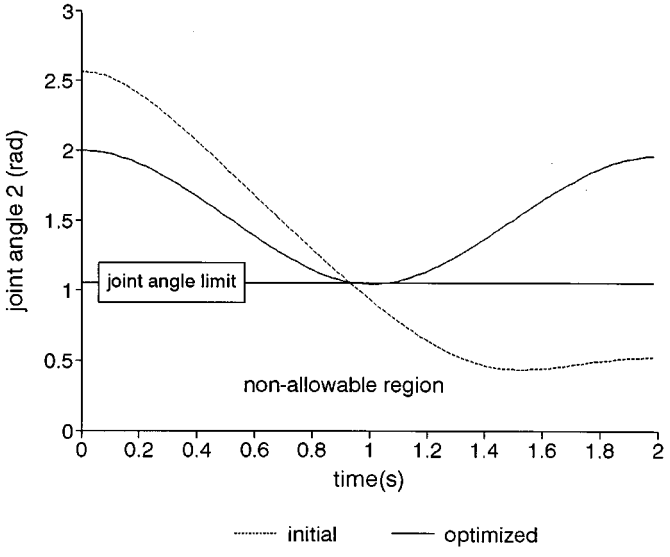

Figure 11. Joint angle vs. time graph for joint 2 (Case 1a Table V)

convergence is not always to the same design. When two or more initial designs, however, converge to the same local optimum solution it is further confirmation that a true local and probable global minimum has been found.

Another observation made is that the constraints sometimes appear to work against each other, especially the torque and joint angle constraints. To satisfy the joint angle constraints the links are made longer and the base position is placed further from the path. To satisfy the torque constraints the design tends to shorten the links and move the base position closer to the path. There is thus a conflict between satisfying the torque and satisfying the joint angle constraints. This may be resolved by increasing the respective penalty parameters at different rates. Even doing so it may sometimes be found that the algorithm fails when these constraints are working against each other, with the algorithm converging to a compromised infeasible solution. It is, in general, difficult to predict where in the design space such conflicts occur and the best way to deal with this problem is to use multiple starting points. The obtained compromised solutions may however still be of practical value since the algorithm succeeds in reducing the larger violations and may reduce the average violations to acceptable levels.

The heuristic procedure to deal with lock-up configurations also worked satisfactorily. Lock-up was only encountered in the case of the minimization of the average required motor torque and/or when joint angle constraints were not imposed. It was found that with the introduction of joint angle constraints the occurrence of lock-up was greatly reduced. The heuristic procedure was always successful in driving the design away from lock-up whenever it occurred.

CONCLUSION

The study shows that the general optimization methodology presented here may successfully be applied to the optimal design of a relative simple manipulator following a straightforward task trajectory. Here both a design which results in minimum average torque requirement for the

prescribed task as well as one that will result in minimum energy usage are achieved. Perhaps more importantly, since it may often be very difficult to guess a feasible design, the optimization procedure developed here ensures, if possible, a feasible and assembable design within the range of deliverable torque of the available motors. Although the example appears to be a relative simple one, it demonstrates the extreme difficulty that may be encountered when handling assembly constraints. In an attempt to minimize the torque requirement an optimization procedure is inclined to drive a design to one which can no longer be assembled at some point along the task trajectory. This effectively makes it impossible to continue the optimization process. Here a procedure is proposed and successfully applied to deal with such 'lock-up trajectories'. It ensures continuation of the optimization process to produce a feasible optimum design.

The optimization methodology proposed here may in principle be easily extended to apply to more complicated manipulators performing more intricate tasks with different design objectives. The only inhibiting factor at present is that the procedure is computationally relatively expensive. This is, amongst others, due to the fact that relative high accuracy is required in the numerical integration which has to be performed to give sufficiently accurate values for the objective function $F(\mathbf{x})$, and because the gradients are calculated by finite differences. This expense becomes more serious as the number of design variables is increased. One may expect however that as more computational power becomes available in future and more use is made of parallel processors, which will allow for the simultaneous computation of gradient components, that the application of the methodology outlined in this paper will become more practical and economic.

REFERENCES

1. A. Sharon, Editorial, *Robotics and Computer Integrated Manufacturing*, **12,** 1–2 (1996).
2. G. A. Gabriele, 'Optimization in mechanisms', in Erdman (ed.), *Modern Kinematics*: *Development in the Last Forty Years*, Chapter 11, Wiley, New York, 1992.
3. V. N. Sohoni and E. J. Haug, 'A state space technique for optimal design of mechanisms', *ASME J. Mech. Des.*, **104,** 792–798 (1982).
4. T. A. Dwarakanah *et al.*, 'Design of articulated manipulators based on kinematic and dynamic criteria', *ASME Mech. Design Conf.*, Vol. DE-45, Tempe Arizona, 1992.
5. J. O. Kim and P. K. Khosla, 'Design of space shuttle tile servicing robot: An application of task based kinematic design', *Proc. IEEE Conf. on Robotics and Automation*, Vol. 3, Atlanta Georgia, 1993.
6. S. Shankar and A. Saraf, 'Singularities in mechanisms—the local tracking problem', *Mech. Mach. Theory*, **30,** 1139–1148 (1995).
7. J. A. Snyman, 'A new and dynamic method for unconstrained minimization', *Appl. Math. Modelling*, **6,** 449–462 (1982).
8. J. A. Snyman, 'An improved version of the original leap-frog dynamic method for unconstrained minimization. LFOP1(b)', *Appl. Math. Modelling*, **7,** 216–218 (1983).
9. P. E. Nikravesh, *Computer-aided Analysis of Mechanical Systems*, Prentice-Hall, Englewood Cliffs, N.J., 1988.
10. E. J. Haug, *Computer-aided Kinematics and Dynamics of Mechanical Systems*, Allyn and Bacon, Boston, 1989.
11. D. F. Berner, 'Optimum design of a planar robotic manipulator', *Masters Thesis*, Department of Mechanical Engineering, University of Pretoria, Pretoria, South Africa, 1996.
12. J. A. Snyman, C. Frangos and Y. Yavin, 'Penalty function solutions to optimal control problems with general constraints via a dynamic optimization method', *Comput. Math. Appl.*, **23,** 47–56 (1992).
13. J. A. Snyman, N. Stander and W. J. Roux, 'A dynamic penalty function method for the solution of structural optimization problems', *Appl. Math. Modelling*, **18,** 453–460 (1994).
14. A. A. Brown, 'Numerical experience with trajectory following methods for unconstrained optimization', *Technical Report 154*, *Hatfield Numerical Optimization Centre*, Hatfield, 1985.
15. J. A. Snyman, P. S. Heyns and P. J. Vermeulen, 'Vibration isolation of a mounted engine through optimization', *Mech. Mach. Theory*, **30,** 109–118 (1995).

